scientific reports

Check for updates

OPEN

Nicotinamide mononucleotide boosts the development of bovine oocyte by enhancing mitochondrial function and reducing chromosome lagging

Shu Hashimoto[1]✉, Udayanga Gamage[2], Yuki Inoue[3], Hisataka Iwata[3] & Yoshiharu Morimoto[2]

Nicotinamide adenine dinucleotide (NAD(H)) and its metabolites function as crucial regulators of physiological processes, allowing cells to adapt to environmental changes such as nutritional deficiencies, genotoxic factors, disruptions in circadian rhythms, infections, inflammation, and exogenous substances. Here, we investigated whether elevated NAD(H) levels in oocytes enhance their quality and improve developmental competence following in vitro fertilization (IVF). Bovine cumulus-oocyte complexes (COCs) were matured in a culture medium supplemented with 0–100 µM nicotinamide mononucleotide (NMN), a precursor of NAD(H). The addition of NMN caused an increase in intracellular NAD(H) and nicotinamide adenine dinucleotide phosphate levels, leading to enhanced competence for development to the blastocyst stage after IVF. The increase in intracellular NAD(H) levels led to changes in the expression of mitochondria function-related genes. As a result, NMN supplementation increased the ratio of MitoTracker Orange fluorescence to nonyl acridine orange fluorescence, as well as adenosine triphosphate levels, while decreasing reactive oxygen species levels in the oocytes. NMN also lowered chromosome lagging during anaphase. These results suggest that increased NAD(H) levels in oocytes following NMN treatment enhances post-fertilization developmental competence through improved mitochondrial function.

Keywords Cattle, Oxidative stress, Meiotic spindle, In vitro embryo production

The in vitro maturation (IVM) of oocytes is a crucial technique for assisted reproductive technology, with extensive related research and clinical applications[1]. It is used not only for human infertility treatment[2]but also for producing mature oocytes in animal reproduction[3]. However, the developmental capacity of embryos produced using IVM oocytes is generally lower than that of their in vivo counterparts, possibly due to inappropriate cytoplasmic conditions[3,4].

Nicotinamide adenine dinucleotide (NADH), the reduced form of NAD^+, was discovered in 1906 as a component enhancing the fermentation rate of yeast[5]. It plays a central role as a hydrogen donor in mitochondrial redox reactions for adenosine triphosphate (ATP) synthesis and reactive oxygen species (ROS) production[6]. Apart from its vital role as a cofactor in energy metabolism, NADH has numerous functions in cellular processes and cellular function regulation, acting as a cofactor or substrate for hundreds of enzymes[7]. NAD^+has been identified as a substrate for enzymes such as sirtuins, poly (ADP-ribose) polymerase (PARP), cluster of differentiation 157 (CD157), CD73, CD38, and sterile alpha and TIR motif containing 1 (SARM1)[8,9,10,11]. Furthermore, NAD^+has been shown to serve as a nucleotide analog in DNA ligation and RNA capping[12,13]. Thus, $NAD^+$and its metabolites contribute to the reorganization of cellular processes through post-synthetic modifications of fundamental biomolecules like DNA, RNA, and proteins in response to various stresses and physiological stimuli[14,15].

A decrease in NAD^+ levels is associated with several diseases, including metabolic and neurodegenerative disorders, and is correlated with aging in rodents and humans. Consequently, the impact of NADH and

[1]Graduate School of Medicine, Osaka Metropolitan University, Osaka 545-8585, Japan. [2]HORAC Grand Front Osaka Clinic, Osaka 530-0011, Japan. [3]Department of Animal Science, Tokyo University of Agriculture, Kanagawa 243-0034, Japan. ✉email: shu@omu.ac.jp

NAD^+(NAD(H)) metabolism on diseases, particularly age-related diseases, has garnered attention[11,13]. In this context, replenishing NAD(H) levels using NAD(H) precursors, such as nicotinamide riboside (NR) or nicotinamide mononucleotide (NMN), has emerged as a significant approach for treating age-related diseases in rodent models. Notably, administering NMN or NR to aged mice improved mitochondrial function in oocytes, reduce the frequency of spindle structure abnormalities, and enhance developmental competence[16,17].

Moreover, culturing isolated cells without NAD(H) precursors, where the salvage pathway for NAD(H) synthesis is not functional, is predicted to decrease NAD^+levels below the physiological requirement. Adding NAD(H) precursors to in vitro cultured porcine oocytes has been shown to increase their maturation[18]. However, the study did not investigate changes in cellular NAD(H) levels, and the mechanism of action underlying the increased rate of parthenogenesis and developmental potential after in vitro fertilization (IVF) remains unclear. The present study aimed to investigate the intracellular changes and improvement in developmental competence following the NMN supplementation of in vitro cultured oocytes.

Results

NMN increased NAD(H) levels in oocytes and improved their ability to develop into blastocysts after IVF

As shown in Fig. 1A, the amount of NAD(H) in oocytes increased significantly ($P < 0.01$) when more than 1 μM NMN was added. The amount of NAD(H) in oocytes also increased significantly when 50 μM NMN was added compared to when 10 μM or less NMN was added ($P < 0.01$). Furthermore, NAD(H), NAD^+, and NADH levels in oocytes cultured with 100 μM NMN were significantly increased compared to those in controls ($P < 0.01$, Fig. 1B-D).

Whether increased NAD(H) levels in oocytes improved their ability to develop into blastocysts was investigated using 10 μM NMN-cultured oocytes. However, the blastocyst formation rate on Day 7 after fertilization did not increase (Figure 1E). Next, IVM culture of oocytes was performed without NMN, with 1 μM NMN, and with 100 μM NMN. The blastocyst formation rate of oocytes supplemented with 100 μM NMN

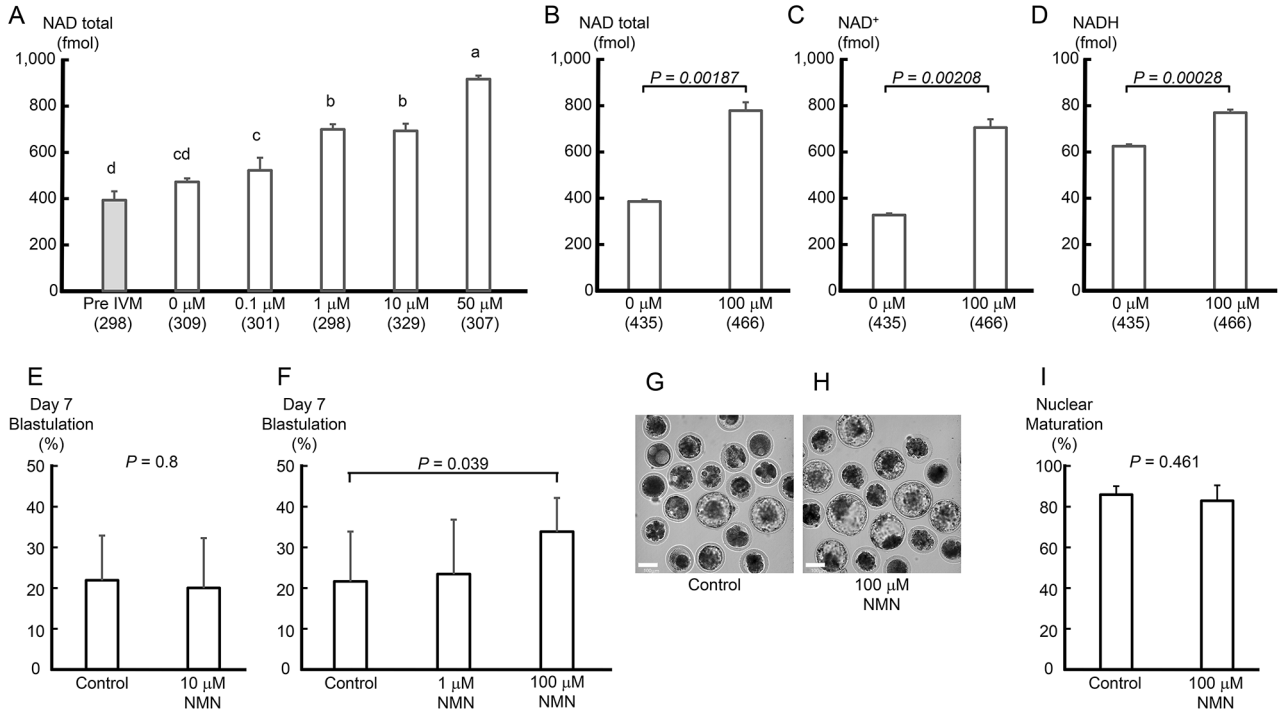

Fig. 1. NMN increased oocyte NAD(H) levels and improved their developmental competence after IVF. (**A**) As the concentration of NMN in the culture medium increased (0–50 μM), NAD(H) levels in the oocytes increased. NMN in the culture medium (100 μM) increased (**B**) total NAD, (**C**) NAD^+, and (**D**) NADH levels in oocytes. Data were obtained from three experimental replicates. (**A-D**) Numbers in parentheses indicate the number of oocytes used in the measurements. (**E**) The addition of NMN (10 μM) to the in vitro oocyte maturation medium did not affect the blastocyst formation rate (blastulation). Data were obtained from 8 repeat experiments using 20 oocytes per trial. (**F**) However, 100 μM NMN to the medium significantly improved the blastulation ($P < 0.05$). Data were obtained from 11 repeat experiments using 20 oocytes per trial. Representative images from Day 7 of embryos cultured in (**G**) 0 and (**H**) 100 μM NMN. The scale bar is 100 μm (G, H). (**I**) The addition of NMN (100 mM) did not affect nuclear maturation. Data were obtained from 5 repeat experiments using 20 oocytes per trial. Data are shown as the mean ± SD. (**A**) $^{a\text{-}d}P < 0.05$ by ANOVA followed by the Tukey–Kramer test. Statistical comparison between two groups was performed using a t-test.

on Day 7 after IVF was significantly improved compared to that of the control ($P < 0.05$, Figure 1F-H). The nuclear maturation rate of oocytes under these conditions was 83% in the NMN-added group and 86% in the control, with no significant difference (Figure 1I).

NMN significantly altered mitochondrial gene expression and enhanced mitochondrial function in oocytes

To understand the mechanism by which the developmental potential of oocytes after IVF was improved by increasing the NAD(H) level, we examined changes in the gene expression patterns in the oocytes uppon adding 100 μM NMN to the oocyte culture. The expression levels of 112 genes increased by more than twofold, and those of 280 genes decreased by less than half, indicating that the gene expression pattern of the oocytes changed drastically (Fig. 2A). In cumulus cells, the expression levels of 204 genes increased by more than twofold and those of 295 genes decreased by less than half.

Since mammalian oocytes, including those of humans, store maternal mRNA in membrane-free compartments with hydrogel-like properties around mitochondria using their membrane potentials[19], we used Mitocarta 3.0 to analyze gene expression changes, focusing on mitochondria. Genes with an absolute fold change value greater than 0 and a p-value less than 0.05 were treated as differentially expressed genes (DEGs). The results showed that in oocytes, the expression of 85 out of 1,136 mitochondria-related genes varied (7.5%, Fig. 2B). In particular, gene expression was upregulated in lipid metabolism, amino acid metabolism, nucleotide metabolism, vitamin metabolism, apoptosis, oxidative phosphorylation, and the mitochondrial central dogma. On the other hand, only 20 genes out of 1,136 showed variable expression in the cumulus cells (1.8%, Suppl. Figure 1). The results indicate that mitochondrial function in oocytes might be greatly affected by elevated intracellular NAD(H) levels.

Since gene expression analysis indicated that mitochondrial function was altered by NMN, we evaluated mitochondrial function by double-staining cells with MitoTracker Orange (MTO) and nonyl acridine orange (NAO) and calculating the ratio of MTO fluorescence to NAO fluorescence. Mitochondrial function in oocytes cultured with 100 μM NMN increased significantly ($P < 0.05$, Fig. 2C, D). Next, when intracellular ATP levels were measured, a trend toward increased ATP levels in oocytes was observed upon adding NMN to the culture medium, particularly when the concentration exceeded 10 μM ($P < 0.01$, Fig. 2E).

NMN increased nicotinamide adenine dinucleotide phosphate (NADP(H): NADPH and NADP$^+$) levels and decreased ROS levels in oocytes

The amount of NADP(H) produced from NAD^+ by NAD^+ kinase (NADK) was examined. Adding 100 μM NMN significantly increased the NADP(H) level in cultured oocytes compared to that in the control ($P < 0.01$, Fig. 3A).

Intracellular NADPH plays an important role in balancing the intracellular redox state via glutathione (GSH)[20]. Therefore, we examined whether elevated intracellular NADPH decreased intracellular ROS. A tendency for intracellular ROS levels to decrease was observed upon adding increasing NMN concentrations to the culture medium, especially above 10 μM ($P < 0.01$, Fig. 3B).

NMN reduced the occurrence of chromosome lagging in anaphase I

Administering NAD^+precursors to aged mice has been shown to improve mitochondrial function in oocytes and ameliorate abnormal spindle structures in meiosis II oocytes[16]. In this study, we investigated whether a similar effect could be achieved by focusing on the frequency of appearance of lagging chromosomes in anaphase I. When immature bovine oocytes were cultured in vitro, a large number of anaphase I oocytes appeared around 18.5 h after the start of culture[21,22], so the cumulus cells were removed from the oocytes at 18 h. The oocytes were fixed at 18.5 h, and the spindle structure was observed. The percentages of oocytes in anaphase I and telophase I were 52% in the control group and 58% in the NMN-treated group (Fig. 4A-D).

The percentage of anaphase I spindles with lagging chromosomes in anaphase I oocytes was 43.9% in the control and 21.4% in the NMN-treated oocytes (Fig. 4E). NMN significantly reduced the frequency of anaphase I spindles with lagging chromosomes ($P < 0.05$).

Discussion

The results of the present study showed that adding NMN, a precursor of NAD^+, to the culture medium increased the amount of NAD(H) and NADP(H) in oocytes (Fig. 5). Oocytes with increased intracellular NAD(H) and NADP(H) levels had a significantly improved ability to develop into blastocysts after IVF. In oocytes with improved developmental potential, the expression pattern of mitochondria-related genes was significantly altered, along with increased mitochondrial membrane potential and ATP levels and decreased ROS amounts. NMN also reduced chromosome segregation errors in meiosis I oocytes.

NAD^+ is continually consumed by three types of enzymes: NAD^+glycohydrolases, the protein deacylase family of sirtuins and PARPs[14,15,23]. These enzymes utilize NAD^+ as a substrate or cofactor and produce nicotinamide (NAM) as a by-product. As such, NAD^+mediates several key biological processes and is constantly in high demand[14,15,23]. To maintain NAD^+levels, NAM can regenerate it via the NAM salvage pathway[14,15,23]; NAD^+ is continuously synthesized, catabolized, and recycled within the cell, ensuring stable intracellular NAD^+ levels. However, isolating cells from tissue and culturing them risks disrupting the balance of mechanisms that maintain stable intracellular NAD^+ levels. We have shown that the addition of NMN, a precursor of NAD^+, to the culture medium increases NAD(H) levels in oocytes. The NAM salvage pathway generates NAD^+ from the NAD^+precursors NAM, NR, and NMN[24,25]. Regarding the uptake of NAD^+ and NMN by cells, some reports argue that NAD^+ and NMN cannot permeate the cell membrane. Instead, nicotinic acid, NAM, NR, tryptophan, and other precursors are thought to be taken up directly into the cell and used for NAD^+biosynthesis[15]. Extracellular

A The number of DEGs obtained for each test plot

Oocyte DEG number	fold change >2	fold change >0	fold change <0	fold change <-2	absolute fold change>2	absolute fold change>0
P value<0.05	112	523	847	280	392	1370
FDR<0.05	0	7	40	5	5	47
CC DEG number	**fold change >2**	**fold change >0**	**fold change <0**	**fold change <-2**	**absolute fold change>2**	**absolute fold change>0**
P value<0.05	204	246	384	295	499	630
FDR<0.05	1	1	4	4	5	5

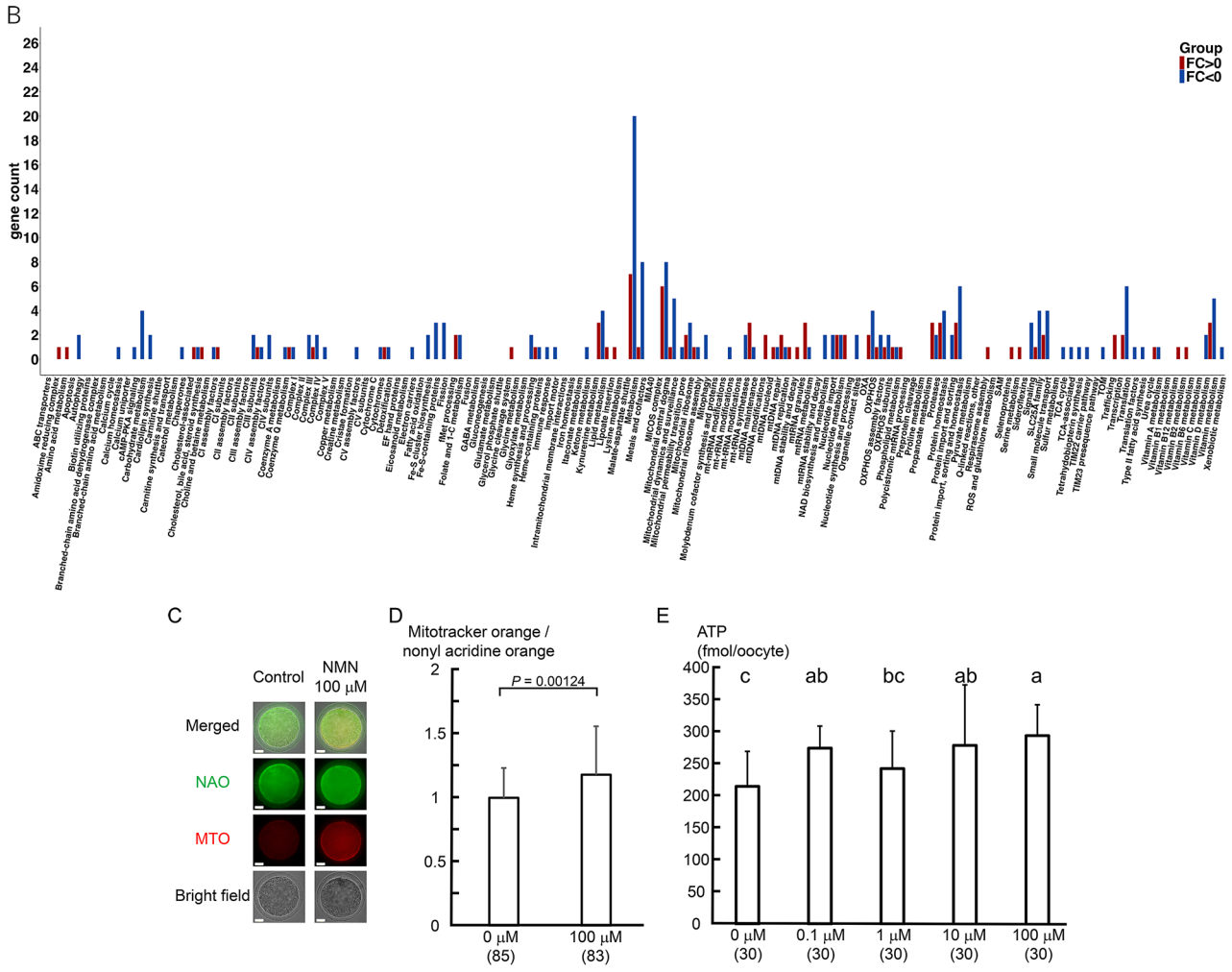

Fig. 2. NMN enhanced mitochondrial function in oocytes. (**A**) Changes in gene expression in oocytes and cumulus cells following NMN treatment (100 μM). The number of differentially expressed genes obtained for each test plot is shown. The expression levels of 112 genes increased by more than twofold and those of 280 genes decreased by less than half, indicating that the gene expression pattern in the oocytes changed drastically. (**B**) The expression of 85 genes among 1,136 mitochondria-related genes varied (7.5%). Genes related to lipid metabolism, amino acid metabolism, nucleotide metabolism, vitamin metabolism, apoptosis, oxidative phosphorylation, and the mitochondrial central dogma were upregulated, and fluctuations in gene expression were observed. (**C**) Mitochondrial activity was evaluated using 0.5 μM MitoTracker Orange (MTO) and 10 μM nonyl acridine orange (NAO). Representative images of MTO and NAO-stained oocytes cultured with or without NMN are shown. The scale bar is 25 μm. (**D**) Mitochondrial function was evaluated by dividing the value obtained by staining identical oocytes with MTO by the value obtained by staining them with NAO. The values were also standardized by dividing each value by a control value measured within the same experiment. In total, 168 oocytes were used to analyze mitochondrial activity in four independent runs. $P < 0.05$ by t-test. (**E**) The ATP level of oocytes was determined as luminescence emitted in an ATP-dependent luciferin–luciferase bioluminescence assay. Ten oocytes per trial were sampled individually from three independent experiments. In total, 150 oocytes were used for the analysis in three independent runs. $P < 0.05$ by ANOVA followed by the Tukey–Kramer test. Numbers in parentheses indicate the number of oocytes used in the measurements.

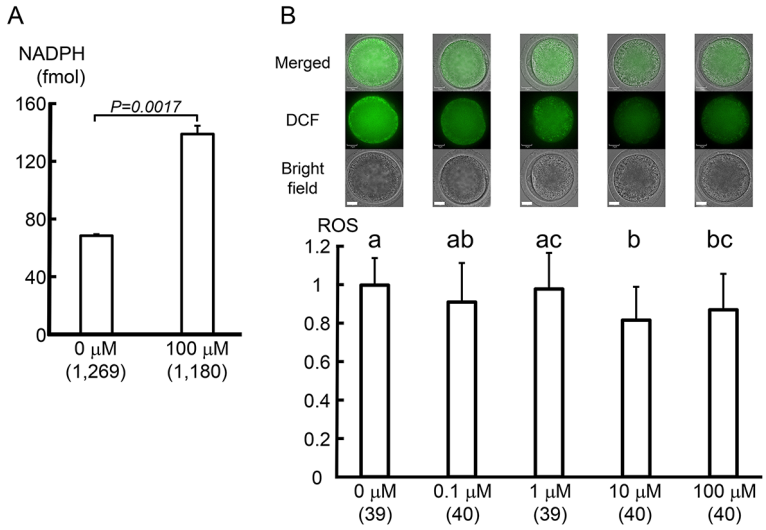

Fig. 3. NMN increased NADP(H) levels and decreased ROS levels in oocytes. (**A**) NADP(H) levels increased in oocytes cultured with 100 μM NMN. A total of 2,449 oocytes was used to analyze NADP(H) values in three independent runs. $P < 0.01$ by *t*-test. (**B**) Oocytes cultured with 0–100 μM NMN were stained with 1 μM H2DCFDA and the amount of hydrogen peroxide (H_2O_2) in the oocytes was compared. A tendency for ROS levels in oocytes to decrease with increasing NMN concentrations in the culture medium, especially at 10 μM NMN or higher, was visible. The experiment was repeated four times, sampling 9–10 oocytes per trial. In total,198 oocytes were used for the analysis in four independent runs. $^{a\text{-}c}P < 0.05$ by ANOVA followed by the Tukey–Kramer test. Numbers in parentheses indicate the number of oocytes used in the measurements. The scale bar is 25 μm.

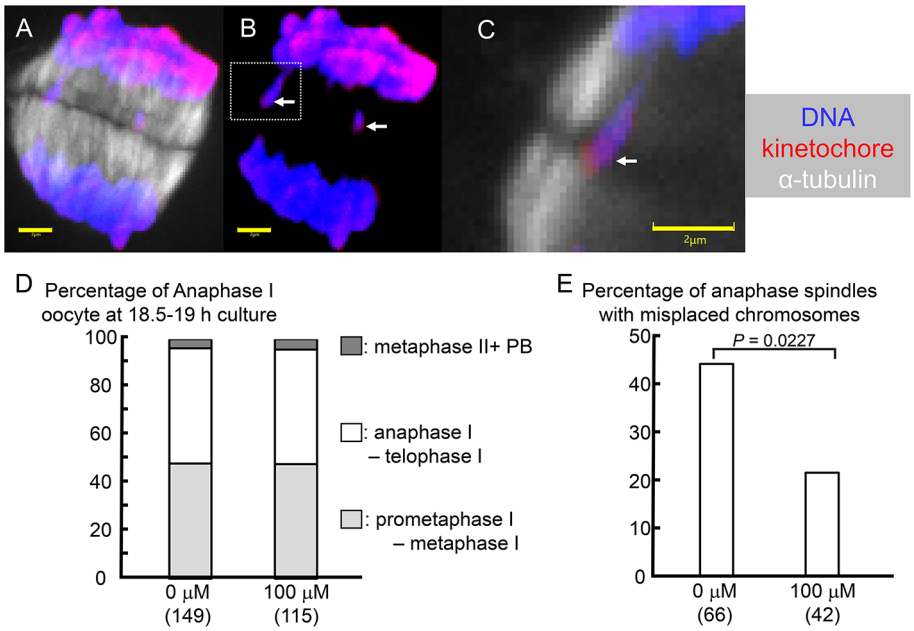

Fig. 4. NMN reduced the occurrence of chromosome lagging in anaphase I**.** (**A, B**) Maximum intensity projections of confocal sections captured every 0.5 μm along the z-axis of anaphase I oocytes cultured without NMN. (**C**) Enlarged view of the area enclosed by the white dashed line in (**B**). Staining: DNA (blue), α-tubulin (white), and kinetochore (red). (**A**, **C**) DNA, α-tubulin, and kinetochore. (**B**) DNA and kinetochore. (**B, C**) The white arrow shows a lagging chromosome. The scale bar is 2 μm. (**D**) Cell cycle of oocytes after 18.5–19 h of culture. (**E**) NMN reduced the occurrence of anaphase I spindle with lagging chromosomes. Numbers in parentheses indicate the number of oocytes used in the measurements. $P < 0.05$ by the chi-square test.

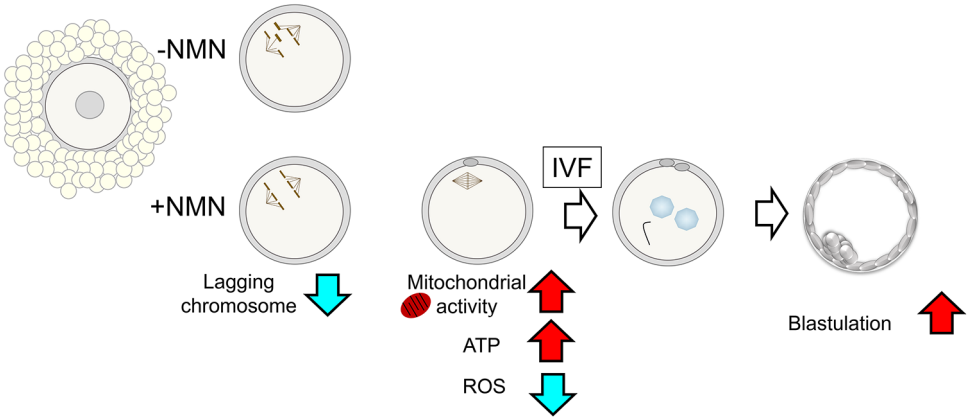

Fig. 5. Scenario of the development capacity of the oocyte cultured with NMN. NMN enhance oocyte quality by improving mitochondrial function, reducing intracellular ROS, and decreasing the risk of chromosomal aberrations.

NMN must be converted to NR by the 5′-nucleotidase CD73 before being taken up intracellularly and then converted back to NMN by nicotinamide riboside kinase 1[26]. However, other reports confirm the presence of a specific NMN transporter, solute carrier family 12 member 8, which is highly expressed in the small intestine and lateral hypothalamus, suggesting that NMN can directly enter the NAD^+biosynthetic pathway[27,28] Our study did not clarify whether oocytes take up NMN directly or take up NMN metabolites, but adding NMN to the culture medium evidently increased their NAD(H) levels. It is also possible that the cumulus cells attached to the oocytes metabolize or absorb NAD^+ precursors; their role in the elevation of NAD(H) levels in oocytes is not yet fully understood, and further studies are needed to clarify the mechanism underlying the NMN-induced elevation of NAD(H) levels in oocytes.

The addition of NMN to the culture medium increased not only NAD(H) but also NADP(H) levels in oocytes, where NAD^+ is directly phosphorylated by NADK, the only enzyme responsible for de novo $NADP^+$synthesis, to generate NADPH[29]. $NADP^+$is synthesized by transferring a phosphate group from ATP to the 2′-hydroxyl group of the adenosine ribose portion of NAD+[29,30]. NADK accounts for 10% of NAD^+consumption[31], and under conditions where NAD^+ levels decline, such as aging or in vitro cell culture, $NADP^+$ levels also decline. Thus, $NADP^+$ levels are directly related to NAD^+ levels, and the two are believed to fluctuate in tandem. In the present study, the amount of ATP, which donates phosphate groups to NAD^+ when $NADP^+$ is synthesized, also increased. Therefore, it is likely that $NADP^+$ levels increased with the increase in NAD^+ levels.

The present study showed that adding NMN to the culture medium increased oocyte mitochondrial function and ATP levels. An increase in oocyte ATP levels in is believed to improve their developmental potential after IVF[32]. On the other hand, ROS are byproducts of energy production in the mitochondrial electron transfer system to generate ATP and are produced in excess when the balance between oxidation and anti-oxidation is disturbed, causing irreversible damage to the ovaries, especially the oocytes[33]. An increase in ROS hinders oxidative phosphorylation and induces telomere shortening and cell apoptosis, thus advancing ovarian senescence[343536]. In our study, adding NMN to the culture medium increased NADP(H) levels in the oocytes, resulting in a rather low ROS level, and no negative effects of increased mitochondrial function were observed. NADP(H) maintains reduced GSH and thioredoxin, thereby preventing excessive oxidative stress and maintaining favorable redox homeostasis[29,373839]. Adding NMN to the culture medium increased NAD(H) and NADP(H) levels in the oocytes, accompanied by improved mitochondrial function and reduced ROS levels. These may have contributed to the increased ability of the oocytes to develop into blastocysts after IVF. Administering NR to aged mice enhanced mitochondrial function and improved mouse oocytes quality[40], and it is very significant that simply adding the NAD^+ precursor to the culture medium had the same effect.

With age, aneuploidy occurs in mouse and human oocytes due to meiotic segregation errors[414243]. Insufficient mitochondrial oxidative phosphorylation in mouse oocytes has been shown to cause meiotic spindle abnormalities[44]. Additionally, inadequate ATP production has been shown to lead to the dysfunction of motor proteins migrating on microtubules, with detrimental consequences for spindle shaping and chromosome segregation, resulting in the generation of aneuploid gametes[45,46]. Administering NR, an NAD^+precursor, may reduce the accumulation of ROS in oocytes from aged individuals, improve spindle assembly, and minimize aneuploidy[47]. The bovine oocytes used in this study were obtained from non-aged individuals and showed no significant abnormalities in spindle structure during the meiotic second division (data not shown). However, the frequency of chromosome lagging in anaphase I and telophase I was relatively high (50%). On the other hand, adding NMN to the culture medium reduced the occurrence of chromosome lagging. Although the appearance of lagging chromosomes does not necessarily result in chromosomal aberrations in oocytes, it does increase the risk thereof[48]. Therefore, adding NMN may have reduced the risk of chromosomal aberration in oocytes and increased the number of fertilized oocytes that develop normally.

These results indicate that the addition of NAD^+ precursors to the oocyte culture medium increases NAD(H) and NADP(H) levels in the oocytes, improves mitochondrial function, increases ATP levels, reduces ROS levels,

reduces chromosome lagging in late meiosis, and ultimately improves post-IVF developmental performance. Our data provide a rationale for applying NMN to improve the efficiency of reproductive medicine and IVF zygote production in domestic animals.

Methods

Experimental design

This study examined whether adding NMN to the culture medium could increase the amount of NAD(H) in the oocyte. Under conditions in which the amount of NAD(H) in the oocytes increased, the developmental potential of the oocytes into blastocysts after IVF was examined for improvements.

To understand the mechanism by which the developmental competence of the oocyte increased, alterations in oocyte gene expression following the addition of NMN were analyzed, with particular attention to the mitochondria. The improvement of oocyte mitochondrial function was assessed by MTO and NAO double staining and ATP values. The amount of NADP(H) in the oocytes was also measured, as NADP(H), which is synthesized from NAD(H), is involved in reducing intracellular ROS. In addition, the effect of NMN on the occurrence of chromosome aberrations in meiosis was investigated. This study was conducted from January 2020 to July 2024.

Oocyte collection and maturation

Bovine ovaries were obtained from Japanese Black cows and heifers, aged around 30 months (between 25 and 36 months), at a local slaughterhouse in Osaka city and transported to the laboratory in saline for 3–5 h at 18–21 °C. Bovine oocytes were collected from follicles (diameter, 2–5 mm) by aspiration using a 21-gauge needle, and oocytes with intact cumulus granulosa cells and evenly granulated cytoplasm (COCs) were selected and randomly assigned to each treatment.

COCs were washed in IVM medium, which consisted of TCM 199 (12,340–030, Gibco, Grand Island, NY, USA), 0.02 mg/ml FSH (Antrin; Kyoritsu, Tokyo, Japan), 1 μg/ml estradiol-17β (E-8875; Sigma-Aldrich, Burlington, MA, USA), 0.1% poly(vinyl alcohol) (PVA-199; Sigma-Aldrich), and 1% (w/v) gentamycin solution (G1397; Sigma-Aldrich)[49]. Each group of 10 COCs was introduced into a 50-μl droplet of IVM medium in a plastic dish covered with mineral oil (M-8416; Sigma-Aldrich) immediately after oocyte collection. The COCs were cultured in IVM culture medium supplemented with 0–100 μM NMN (N3501-25MG; Sigma-Aldrich) for 21 h at 39 °C under 5% CO_2 in air at high humidity. Following the culture, 20 oocytes per treatment were fixed in ethanol: acetic acid (3:1), stained with aceto-orcein (1%w/v), and observed under a phase contrast microscope.

Transcriptome analyses

A total of 486 COCs were used after culture in 100 μM NMN. Total RNA was extracted using the RNAqueous-Micro Total RNA Isolation Kit (Thermo Fisher Scientific, Foster City, CA, USA) from oocytes or cumulus cells separately after their isolation. Cumulus cells were removed from COCs by processing for 8 min using a vortex mixer at approximately 2,800 rpm/min 21 h after the start of the culture and recovered after centrifuging the cell suspension. The RNA of oocytes and cumulus cells without exposure to NMN was also extracted from 506 COCs as a reference. RNA from approximately 160 COCs was collectively used as a single template for three replicates.

RNA was extracted using the RNAqueous™ Total RNA Isolation Kit (AM1912; Thermo Fisher Scientific), and RNA quality and concentration were measured using Bioanalyzer 2100 (Agilent Technologies, Palo Alto, CA, USA). The mean and SEM of RNA integrity numbers were 7.133 ± 0.067 for control oocytes, 7.067 ± 0.033 for NMN oocytes, 7.8 ± 0.854 for control cumulus cells, and 8.1 ± 0.208 for NMN cumulus cells.

Libraries were prepared using the NEBNext Single Cell/Low Input RNA Library Prep kit (New England Biolabs, Ipswich, MA, USA). Three samples from each group were sequenced as 100 bp reads (single reads) on a NextSeq1000 (Illumina, San Diego, CA, USA). Image analysis, base calling, quality filtering, and Fastq file creation were performed using RTA version 2.4.11 and bcl2fastq2 v2.20.0.422 (Illumina), following the manufacturer's instructions. Sequence data were filtered using CLC workbench (v.23.0; Qiagen, Hilden, Germany) to discard adapter sequences, ambiguous nucleotides, and low-quality sequences. A quality check was repeated to confirm the above deletions. The mean and SEM of reads were as follows: control oocytes: $29{,}597{,}294 \pm 1{,}584{,}188$; NMN oocytes: $29{,}224{,}101 \pm 1{,}158{,}399$; control cumulus cells: $26{,}210{,}283 \pm 909{,}769$; and NMN cumulus cells: $28{,}299{,}207 \pm 101{,}908$. The remaining sequence data were aligned to *Bos taurus* reference data (ARS204 URD 1.2.108) and sequence reads were counted. Gene expression values were evaluated using transcripts per kilobase million (TPM), and genes with an absolute fold change of at least 2 were defined as significant DEGs.

Annotation/principal component analysis (PCA)

Mapped samples were annotated for each experimental category of oocytes and cumulus cells using a two-group comparison method. The volcano plots of oocytes and cumulus cells are shown in Suppl. Figure 2A, B. The data were deposited in the DDBJ BioProject database under the BioProject accession number: PRJDB18511.

In addition, Mitocarata 3.0 (https://www.broadinstitute.org/mitocarta/mitocarta30-inventory-mammalian-mitochondrial-proteins-and-pathways) was used to extract mitochondria-related genes among the DEGs. Mitocarata is an encyclopedic catalog of human/mouse mitochondria-related genes and their functions. Because the taxonomy of *Bos taurus* was not available in Mitocarata, the gene list of *Homo sapiens* was used as background and converted with *Bos taurus* orthologs. Ingenuity® Pathway Analysis was used to determine the number of known targets of each transcription regulator in the list of DEGs, and a statistical test was performed to consider their significance. Fisher's exact test was used to statistically analyze gene set enrichment in each functional category.

Mitochondrial function and ROS level in oocytes

COCs were denuded with a vortex mixer 21 h after the start of the culture. Denuded oocytes were incubated with 0.5 µM MTO CM-H2TMRos (M-7511; Life Technology, Carlsbad, CA, USA) and 10 µM NAO (A1372; Thermo Fisher Scientific) for 30 min in PVA-199 at 39 °C under 5% CO_2, 5% O_2, and 90% N_2 and then washed three times in bicarbonate-buffered synthetic oviduct fluid with amino acids (SOFaa). Stained oocytes were transferred to a 3-µL droplet of SOFaa on a glass-bottomed culture dish (P35G-0–14-C; MatTek Corporation, Ashland, MA, USA). Microscopic images were obtained using a confocal microscope (CLM, CV1000; Yokogawa Electronic, Tokyo, Japan) at 40 × and 39 °C under 5% CO_2, 5% O_2, and 90% N_2, and fluorescence intensity in the equatorial plane of the oocytes was measured using ImageJ (http://imagej.nih.gov/ij/). Mitochondrial function was evaluated by dividing the value obtained by staining identical oocytes with MTO by the value obtained by staining them with NAO. The values were also standardized by dividing each value by a control value measured within the same experiment. In this study, a total of 168 oocytes were used to analyze mitochondrial activity in four independent runs.

Denuded oocytes were washed in Ca^{2+}- and Mg^{2+}-free PBS (PBS (−)) supplemented with 0.1% PVA (PVA – PBS) and stained with 1 µM H2DCFDA (D399; Thermo Fisher Scientific) PVA-PBS for 10 min at room temperature (RT) under light shielding as previously described[50]. Just before the start of each experiment, fresh H2DCFDA was prepared at 1 µM in PVA – PBS from a stock solution (1 mM in dimethyl sulfoxide). Stained oocytes were washed in PVA – PBS to remove traces of the dye and transferred to a 3-µL droplet of PVA – PBS on a glass-bottomed culture dish. Microscopic images were obtained using the CLM at 40 × at RT in air, and fluorescence intensity in the equatorial plane of the oocytes was measured using ImageJ (http://imagej.nih.gov/ij/). In this study, a total of 198 oocytes were used to analyze ROS content in four independent runs. The fluorescence intensity of each sample was divided by the mean intensity of the control in each run and compared.

Oocyte ATP levels

The ATP level of oocytes was determined as luminescence emitted in an ATP-dependent luciferin–luciferase bioluminescence assay (ATP assay kit; Toyo-Inc., Tokyo, Japan). Serial dilutions of the ATP standard ranging from 100 nM to 0.01 pM were prepared, and a standard curve was prepared based on the relative light intensity of the serial dilution standard (log luminescence vs. log[ATP]). The standard curve was used to calculate the ATP level of the samples. Samples were measured in duplicate and the mean was calculated. To prepare each sample, one oocyte was added to 50 µL of distilled water. The oocyte was lysed and the luminescence was measured immediately using a luminometer (Gene Light 55; Microtec, Funabashi, Japan). Ten oocytes per trial were sampled individually from three independent experiments. A total of 150 oocytes were used in three independent runs.

Spindle structure analysis in anaphase I

Cumulus cells were removed from oocytes 18 h after the start of the maturation culture. The oocytes were then washed in PVA-PBS and fixed in 2% (v/v) paraformaldehyde (167–25,981; FUJIFILM Wako Pure Chemical Corporation, Osaka, Japan) at 37 °C for 30 min. Before incubation with the primary antibody, lipid droplets in bovine oocytes were cleared with 4,000 U/ml lipase from *Candida rugose* (Thermo Fisher Scientific) in 400 mM NaCl, 50 mM Tris (pH 7.2), 5 mM $CaCl_2$, and 0.2% sodium taurocholate supplemented with ethylenediaminetetraacetic acid-free Protease Inhibitor Cocktail (11,836,170,001; Merck KGaA, Darmstadt, Germany) at 37 °C for 30 min as previously described[51] with some modifications. Fixed oocytes were washed in PVA-PBS containing 3% (w/v) BSA (A7638; Sigma-Aldrich) and 0.2% (v/v) Triton-X 100 (BSA–PBS; Sigma-Aldrich). The oocytes were then triple-stained to visualize chromosomal behavior. The samples were incubated in a solution of primary human anti-centromere antibodies (1:100, 15–234; Antibodies Inc., Davis, CA, USA) overnight at 4 °C to identify the kinetochore. After being washed in BSA–PBS, they were incubated in alpaca anti-rabbit/human IgG (1:250, Nano-Secondary® alpaca anti-rabbit/human IgG, recombinant VHH, Alexa Fluor® 568; Proteintech Japan, Inc., Tokyo, Japan), Alexa488®-conjugated mouse anti-α-tubulin (1:250, 322,588; Thermo Fisher Scientific), and 10 µg/ml of bisbenzimide H 33,342 trihydrochloride (Hoechst 33,342, 591–01,721; FUJIFILM Wako Pure Chemical Corporation) overnight at 4 °C. After being washed in BSA–PBS, they were mounted on slides under a coverslip. The samples were examined with the CLM equipped with a 100 × oil immersion lens. Confocal image analysis was typically accomplished by capturing a z-series stack of 0.5-µm-thick optical sections encompassing the entire spindle (Fig. 4A-C). In this study, 177 oocytes were used for spindle morphology analysis in four independent runs.

IVF and culture

IVF and culture were performed as described previously[49]. Briefly, freeze-thawed spermatozoa from a Holstein bull were centrifugally washed for 20 min. at 500G in discontinuous 45% and 90% Percoll solutions (P1644; Sigma-Aldrich). Matured oocytes were inseminated with the washed spermatozoa (1×10^6 cells/ml) in a glucose-free defined medium supplemented with 10 µg/ml of heparin (H-3393; Sigma-Aldrich). IVF was performed at 39 °C under 5% CO_2 in air at high humidity. The oocytes were completely released from the attached sperm using vortex agitation at 2,800 rpm/min for 7 min, 6 h after IVF. Denuded presumptive zygotes were cultured in SOFaa supplemented with 3 mg/ml of BSA (017–15,146; FUJIFILM Wako Pure Chemical Corporation) and 1% (w/v) antibiotic-mycotic solution[49]. Then, 20 of these presumptive zygotes were placed in 50 µl of SOFaa and cultured at 39 °C under 5% CO_2, 5% O_2, and 90% N_2 with high humidity. Development to the blastocyst stage was examined under a stereomicroscope (60 ×) 168 h (Day 7) after IVF. The blastocyst formation rate was calculated by dividing the number of blastocysts by the number of presumptive zygotes cultured.

Statistical analysis

Differences between the two groups were analyzed using the unpaired Student's t-test for embryo development or chi-square test for the occurrence of chromosome lagging. When more than two groups were compared, analysis of variance (ANOVA) followed by the Tukey–Kramer test was used. Normality and homogeneity of variances were confirmed by the Shapiro–Wilk and Levene tests, respectively, before parametric analyses (t-test and ANOVA) were run. The data are shown as the mean ± SD. A p-value less than 0.05 was considered significant.

Data Availability

The data that support the findings of this study have been deposited in the DDBJ BioProject database under the BioProject accession number: PRJDB18511.

Received: 13 August 2024; Accepted: 26 November 2024
Published online: 02 January 2025

References

1. Gilchrist, R. B. & Smitz, J. Oocyte in vitro maturation: physiological basis and application to clinical practice. *Fertil. Steril.* **119**, 524–539. https://doi.org/10.1016/j.fertnstert.2023.02.010 (2023).
2. Trounson, A., Wood, C. & Kausche, A. In-vitro maturation and the fertilization and developmental competence of oocytes recovered from untreated polycystic ovarian patients. *Fertil. Steril.* **62**, 353–362. https://doi.org/10.1016/s0015-0282(16)56891-5 (1994).
3. Leibfried-Rutledge, M. L., Crister, E. S., Eyestone, W. H., Northey, D. L. & First, N. L. Development potential of bovine oocytes matured in vitro or in vivo. *Biol. Reprod.* **36**, 376–383. https://doi.org/10.1095/biolreprod36.2.376 (1987).
4. Sirard, M. A. & Blondin, P. Oocyte maturation and IVF in cattle. *Anim. Reprod. Sci.* **42**, 417–426. https://doi.org/10.1016/0378-4320(96)01518-7 (1996).
5. Harden, A. and Young, W.J. (1906). The alcoholic ferment of yeast-juice part II.–the coferment of yeast-juice. Proc. R. Soc. Lond. B Biol. Sci. 78, 7. https://doi.org/10.1098/rspb.1906.0070
6. Warburg, O. & Christian, W. J. B. Z. Pyridin, the hydrogen-transferring component of the fermentation enzymes (pyridine nucleotide). *Biochem. Z.* **287**, 291–328 (1936).
7. Sahar, S., Nin, V., Barbosa, M. T., Chini, E. N. & Sassone-Corsi, P. Altered behavioral and metabolic circadian rhythms in mice with disrupted NAD^+ oscillation. *Aging* **3**, 794–802. https://doi.org/10.18632/aging.100368 (2011).
8. Chambon, P., Weill, J. D. and Mandel, P. (1963). Nicotinamide mononucleotide activation of new DNA-dependent polyadenylic acid synthesizing nuclear enzyme. Biochem. Biophys. Res. Commun. 11, 39–43. doi; https://doi.org/10.1016/0006-291x(63)90024-x
9. Frye, R. A. Characterization of five human cDNAs with homology to the yeast SIR2 gene: Sir2-like proteins (sirtuins) metabolize NAD and may have protein ADP-ribosyltransferase activity. *Biochem. Biophys. Res. Commun.* **260**, 273–279. https://doi.org/10.1006/bbrc.1999.0897 (1999).
10. Imai, S., Armstrong, C. M., Kaeberlein, M. & Guarente, L. Transcriptional silencing and longevity protein Sir2 is an NAD-dependent histone deacetylase. *Nature* **403**, 795–800. https://doi.org/10.1038/35001622 (2000).
11. Landry, J. et al. The silencing protein SIR2 and its homologs are NAD-dependent protein deacetylases. *Proc. Natl Acad. Sci. USA* **97**, 5807–5811. https://doi.org/10.1073/pnas.110148297 (2000).
12. Bird, J. G. et al. The mechanism of RNA 5' capping with NAD^+, NADH and desphospho-CoA. *Nature* **535**, 444–447. https://doi.org/10.1038/nature18622 (2016).
13. Chen, S. H. & Yu, X. Human DNA ligase IV is able to use NAD^+ as an alternative adenylation donor for DNA ends ligation. *Nucleic Acids Res.* **47**, 1321–1334. https://doi.org/10.1093/nar/gky1202 (2019).
14. Xie, N. et al. NAD^+ metabolism: pathophysiologic mechanisms and therapeutic potential. *Signal Transduct Target Ther.* **5**, 227. https://doi.org/10.1038/s41392-020-00311-7 (2020).
15. Covarrubias, A. J., Perrone, R., Grozio, A. & Verdin, E. NAD^+ metabolism and its roles in cellular processes during ageing. *Nat. Rev. Mol. Cell Biol.* **22**, 119–141. https://doi.org/10.1038/s41580-020-00313-x (2021).
16. Bertoldo, M. J., Listijono, D. R., Ho, W. J., Riepsamen, A. H, Goss, D. M., Richani, D., Jin, X. L., Mahbub, S., Campbell, J. M., and Habibalahi, A. et al., (2020). NAD^+ Repletion Rescues Female Fertility during Reproductive Aging. Cell Rep. doi; 30:1670–1681. https://doi.org/10.1016/j.celrep.2020.01.058
17. Miao, Y., Cui, Z., Gao, Q., Rui, R. & Xiong, B. Nicotinamide Mononucleotide Supplementation Reverses the Declining Quality of Maternally Aged Oocytes. *Cell Rep.* **4**(32), 107987. https://doi.org/10.1016/j.celrep.2020.107987 (2020).
18. Pollard, C. L., Gibb, Z., Hawdon, A., Swegen, A. & Grupen, C. G. Supplementing media with NAD^+ precursors enhances the in vitro maturation of porcine oocytes. *J. Reprod. Dev.* **67**, 319–326. https://doi.org/10.1262/jrd.2021-080 (2021).
19. Cheng, S., Altmeppen, G., So, C., Welp, L. M., Penir, S., Ruhwedel, T., Menelaou, K., Harasimov, K., Stützer, A., and Blayney, M. et al., (2022). Mammalian oocytes store mRNAs in a mitochondria-associated membraneless compartment. Science. 378:eabq4835. https://doi.org/10.1126/science.abq4835
20. Aslund, F., Berndt, K. D. & Holmgren, A. Redox potentials of glutaredoxins and other thiol-disulfide oxidoreductases of the thioredoxin superfamily determined by direct protein-protein redox equilibria. *J. Biol. Chem.* **272**, 30780–30786. https://doi.org/10.1074/jbc.272.49.30780 (1997).
21. Hashimoto, S., Minami, N., Takakura, R. & Imai, H. Bovine immature oocytes acquire developmental competence during meiotic arrest in vitro. *Biol. Reprod.* **66**, 1696–1701. https://doi.org/10.1095/biolreprod66.6.1696 (2002) (**PMID: 12021049**).
22. Hashimoto, S. et al. Mitochondrial function in immature bovine oocytes is improved by an increase of cellular cyclic AMP. *Sci. Rep.* **9**, 5167. https://doi.org/10.1038/s41598-019-41610-6 (2019).
23. Chu, X. & Raju, R. P. Regulation of NAD^+ metabolism in aging and disease. *Metabolism.* **126**, 154923. https://doi.org/10.1016/j.metabol.2021.154923 (2021).
24. Chi, Y. & Sauve, A. A. Nicotinamide riboside, a trace nutrient in foods, is a vitamin B3 with effects on energy metabolism and neuroprotection. *Curr. Opin. Clin. Nutr. Metab. Care* **16**, 657–661. https://doi.org/10.1097/MCO.0b013e32836510c0 (2013).
25. Sorrentino, V. et al. Enhancing mitochondrial proteostasis reduces amyloid-β proteotoxicity. *Nature.* **552**, 187–193. https://doi.org/10.1038/nature25143 (2017).
26. Ratajczak, J. et al. NRK1 controls nicotinamide mononucleotide and nicotinamide riboside metabolism in mammalian cells. *Nat. Commun.* **7**, 13103. https://doi.org/10.1038/ncomms13103 (2016).
27. Grozio, A. et al. Slc12a8 is a nicotinamide mononucleotide transporter. *Nat Metab.* **1**, 47–57. https://doi.org/10.1038/s42255-018-0009-4 (2019).
28. Ito, N. et al. Slc12a8 in the lateral hypothalamus maintains energy metabolism and skeletal muscle functions during aging. *Cell. Rep.* **40**, 111131. https://doi.org/10.1016/j.celrep.2022.111131 (2022).
29. Ying, W. NAD^+/NADH and $NADP^+$/NADPH in cellular functions and cell death: Regulation and biological consequences. *Antioxid. Redox Signal* **10**, 179–206. https://doi.org/10.1089/ars.2007.1672 (2008).

30. Agledal, L., Niere, M. & Ziegler, M. The phosphate makes a difference: Cellular functions of NADP. *Redox Rep.* **15**, 2–10. https://doi.org/10.1179/174329210X12650506623122 (2010).
31. Liu, L. et al. Quantitative Analysis of NAD Synthesis-Breakdown Fluxes. *Cell Metab.* **1**, 1067-1080.e5. https://doi.org/10.1016/j.cmet.2018.03.018 (2018).
32. van Blerkom, J., Davis, P. W. & Lee, J. ATP content of human oocytes and developmental potential and outcome after in-vitro fertilization and embryo transfer. *Hum. Reprod.* **10**, 415–424. https://doi.org/10.1093/oxfordjournals.humrep.a135954 (1995).
33. Ju, W. et al. Mechanisms of mitochondrial dysfunction in ovarian aging and potential interventions. *Front. Endocrinol.* **15**, 1361289. https://doi.org/10.3389/fendo.2024.1361289 (2024).
34. Wang, L. et al. Oxidative stress in oocyte aging and female reproduction. *J. Cell. Physiol.* **236**, 7966–7983. https://doi.org/10.1002/jcp.30468 (2021).
35. Agarwal, A., Gupta, S., Sekhon, L. & Shah, R. Redox considerations in female reproductive function and assisted reproduction: from molecular mechanisms to health implications. *Antioxid. Redox. Signal.* **10**, 1375–1403. https://doi.org/10.1089/ars.2007.1964 (2008).
36. Sun, J. et al. Decreased expression of IDH1 by chronic unpredictable stress suppresses proliferation and accelerates senescence of granulosa cells through ROS activated MAPK signaling pathways. *Free. Radic. Biol. Med.* **169**, 122–136. https://doi.org/10.1016/j.freeradbiomed.2021.04.016 (2021).
37. Xiao, W., Wang, R. S., Handy, D. E. & Loscalzo, J. NAD(H) and NADP(H) Redox Couples and Cellular Energy Metabolism. *Antioxid. Redox Signaling.* **28**, 251–272. https://doi.org/10.1089/ars.2017.7216 (2018).
38. Xu, D., Li, X., Shao, F., Lv, G., Lv, H., Lee, J. H., Qian, X., Wang, Z., Xia, Y., and Du, L. et al. (2019). The protein kinase activity of fructokinase A specifies the antioxidant responses of tumor cells by phosphorylating p62. Sci. Adv. 5, eaav4570. https://doi.org/10.1126/sciadv.aav4570
39. Cao, X., Wu, L., Zhang, J. & Dolg, M. Density functional studies of coenzyme NADPH and its oxidized form NADP(+): structures, UV–Vis spectra, and the oxidation mechanism of NADPH. *J. Comput. Chem.* **41**, 305–316. https://doi.org/10.1002/jcc.26103 (2020).
40. Yang, Q. et al. Increasing ovarian NAD^+ levels improve mitochondrial functions and reverse ovarian aging. *Free. Radic. Biol. Med.* **156**, 1–10. https://doi.org/10.1016/j.freeradbiomed.2020.05.003 (2020).
41. Chiang, T., Schultz, R. M. & Lampson, M. A. Meiotic origins of maternal age-related aneuploidy. *Biol. Reprod.* **86**, 1–7. https://doi.org/10.1095/biolreprod.111.094367 (2012).
42. Nagaoka, S. I., Hassold, T. J. & Hunt, P. A. Human aneuploidy: mechanisms and new insights into an age-old problem. *Nat. Rev. Genet.* **13**, 493–504. https://doi.org/10.1038/nrg3245 (2012).
43. Herbert, M., Kalleas, D., Cooney, D., Lamb, M. & Lister, L. Meiosis and maternal aging: insights from aneuploid oocytes and trisomy births. *Cold. Spring. Harb. Perspect. Biol.* **7**, a017970. https://doi.org/10.1101/cshperspect.a017970 (2015).
44. Zhang, X., Wu, X. Q., Lu, S., Guo, Y. L. & Ma, X. Deficit of mitochondria-derived ATP during oxidative stress impairs mouse MII oocyte spindles. *Cell. Res.* **16**, 841–850. https://doi.org/10.1038/sj.cr.7310095 (2006).
45. Eichenlaub-Ritter, U. Oocyte ageing and its cellular basis. *Int. J. Dev. Biol.* **56**, 841–852. https://doi.org/10.1387/ijdb.120141ue (2012).
46. Schon, E. A. et al. Chromosomal non-disjunction in human oocytes: is there a mitochondrial connection?. *Hum. Reprod.* **15**, 160–172. https://doi.org/10.1093/humrep/15.suppl_2.160 (2000).
47. Pollard, C. L., Younan, A., Swegen, A., Gibb, Z. & Grupen, C. G. Insights into the NAD^+ biosynthesis pathways involved during meiotic maturation and spindle formation in porcine oocytes. *J. Reprod. Dev.* **68**, 216–224. https://doi.org/10.1262/jrd.2021-130 (2022).
48. So, C., Menelaou ,K., Uraji, J., Harasimov, K., Steyer, A.M., Seres, K.B., Bucevičius, J., Lukinavičius, G., Möbius, W., Sibold, C. et al. (2022). Mechanism of spindle pole organization and instability in human oocytes. Science. 375, eabj3944. https://doi.org/10.1126/science.abj3944
49. Hashimoto, S. et al. Effects of cumulus cell density during in vitro maturation of the developmental competence of bovine oocytes. *Theriogenology.* **49**, 1451–1463. https://doi.org/10.1016/s0093-691x(98)00091-0 (1998).
50. Hashimoto, S., Minami, N., Yamada, M. & Imai, H. Excessive concentration of glucose during in vitro maturation impairs the developmental competence of bovine oocytes after in vitro fertilization: relevance to intracellular reactive oxygen species and glutathione contents. *Mol. Reprod. Dev.* **56**, 520–526. https://doi.org/10.1002/1098-2795(200008)56:4%3c520::AID-MRD10%3e3.0.CO;2-0 (2000).
51. So, C., Seres, K.B., Steyer, A.M., Mönnich, E., Clift, D., Pejkovska, A., Möbius, W., Schuh, M. (2019). A liquid-like spindle domain promotes acentrosomal spindle assembly in mammalian oocytes. Science.;364, eaat9557. https://doi.org/10.1126/science.aat9557

Acknowledgements

Part of this work was supported by a grant from the Japan Society for the Promotion of Science (KAKENHI 23K08805 to S.H.), and a Cooperative Research Grant of the Genome Research for BioResources, NODAI Genome Research Center, Tokyo University of Agriculture (to S.H. and H.I.). The authors thank the Genetics Hokkaido Association for the donation of frozen bull sperm, and Cambridge Proofreading Team (https://proofreading.org) for editing a draft of this manuscript.

Author contributions

S.H. designed the experiment, interpreted the results, and wrote the manuscript. S.H. and G.U. measured NAD(H), NADP(H), ROS, and ATP contes. S.H., Y.I. and H.I. performed the transcriptome analysis. Y.M. supervised the project.

Funding

Japan Society for the Promotion of Science,23K08805

Competing interests

The authors declare no competing interests.

Additional information

Supplementary Information The online version contains supplementary material available at https://doi.org/10.1038/s41598-024-81393-z.

Correspondence and requests for materials should be addressed to S.H.